

Influence of firing parameters on phase composition of raw glazes

Linda Fröberg^a, Thomas Kronberg^b, Leena Hupa^{a,*}, Mikko Hupa^a

^a Process Chemistry Centre, Åbo Akademi University, Turku, Finland

^b Ido Bathroom Ltd., Sanitec Group, Ekenäs, Finland

Available online 30 June 2006

Abstract

Raw glazes are well suited for glazes fired traditionally at high top temperatures. Final phase composition of these glazes is assumed to be controlled by nucleation and growth of crystals in the melt. At shorter firing cycles the phase composition of glazes is likely to be restricted by the limited reaction time. In this work the influence of firing cycle and glaze composition on final glaze phase composition was studied. Fifteen experimental raw glazes were fired at short, intermediate and long cycles. Crystalline phases developed in the surfaces were identified with X-ray diffraction and SEM/EDXA. Sintering behaviour of the glazes was studied with hot stage microscopy. Compositional dependence for two typical temperatures from sintering curves was established. The results indicate that the phase composition strongly depends on the firing cycle. Crystalline phases in fast-fired glazes were intermediate products of first raw material reactions, diopside, wollastonite and pseudowollastonite. Traditional firing favours feldspar formation.

© 2006 Elsevier Ltd. All rights reserved.

Keywords: Firing; Sintering; Microstructure-final; Surface; Glazes

1. Introduction

Raw glazes are cost-effective alternatives for dense ceramics fired at high top temperatures. Raw glazes are commonly used for sanitaryware and porcelain, and also for frost resistant floor tiles. Nowadays tiles are often fast-fired for less than 90 min, while the other products undergo a traditional firing cycle of several hours. When choosing a batch formulation to achieve a glazed surface with desired properties both the reaction kinetics of the raw materials and the high temperature properties of the glaze have to be understood. At short firing cycles the limited time suggests that batch reactions are not always completed. Thus understanding the reaction kinetics is of utmost importance to be able to control the final glaze phase composition and thus the surface properties.

In traditional firing the surface composition of glazes is often controlled mainly by viscosity of the melt. During post-sintering crystalline phases according to equilibrium conditions nucleate and grow in the melt. However, the high viscosity of most glaze melts effectively prevents crystallization of phases typical for the lower temperature ranges. The firing requirements set up

by the ceramic body composition together with the raw glaze make up a complex system, which often is mastered by long-term process knowledge, or by trial and error. In laboratory scale hot stage microscopy (HSM) has been widely used to study the sintering process of fritted and raw glazes.^{1–10} Nucleation and crystallization of glazes and glass–ceramics is widely reported in literature, but mostly for fritted compositions or homogeneous glasses.^{11–20} When using raw glazes several different processes take place during the firing cycle, e.g. decomposition of raw materials, chemical reactions giving either crystalline or glassy products, and melting followed by nucleation and crystallization of the melt. The use of raw glazes on traditionally fired products is a well-established practice. However, the behaviour of raw glazes at short firing cycles is still poorly reported in literature.

In this work, the effect of glaze composition and firing conditions on the final phase compositions developed in the fired glaze is studied. Also compositional dependence for two typical temperatures from sintering curves was established. This knowledge offers a possibility to tailor glazes with desired phase compositions.

2. Experimental

The experimental glazes were ball-milled from commercial grade raw materials, cf. Table 1. The feldspar used consists

* Corresponding author at: Biskopsgatan 8, FI-20500 Turku, Finland.
Tel.: +358 215 4563; fax: +358 215 4962.
E-mail address: leena.hupa@abo.fi (L. Hupa).

Table 1
Raw material compositions of the experimental glazes (wt.%)

Glaze	Kaolin	Feldspar	Dolomite	Limestone	Quartz	Corundum
1	6	74.6	14.5	0	0	4.9
2	8	26	15	17.8	13	20.2
3	8	26.2	15	17.7	0.3	32.8
4	5	42.5	14.5	17	0	21
5	5	27.7	0	27	1.4	38.9
6	5.5	25.9	0	43	0.9	24.7
7	5	26.9	7.5	22.6	14.3	23.7
8	5	52.9	8.4	2.85	11.6	19.25
9	5	43	0	41.5	0	10.5
10	5	78	0	7.5	7.55	1.95
11	8	47.95	7.4	22.1	3	11.55
12	8	27.2	15.4	0	0.6	48.8
13	5	45.5	0	42.75	3.7	3.05
14	5	72.8	15	0	7.2	0
15	5	76.6	8.43	2.54	7.43	0

Table 2
Oxide compositions of the experimental glazes (wt.%)

Glaze	Na ₂ O	K ₂ O	MgO	CaO	Al ₂ O ₃	SiO ₂
1	4.6	5.4	3.5	5.6	17.5	63.5
2	1.8	2.2	4	17.5	25	49.5
3	1.8	2.3	4	17.4	10.1	64.5
4	2.8	3.4	3.8	16.8	11.7	61.4
5	1.8	2.3	0.1	17.4	10	68.4
6	1.8	2.3	0.2	29.9	10	55.9
7	1.8	2.2	2	17.6	24.9	51.5
8	3.2	3.8	2	5	25	61.1
9	3	3.6	0.2	28.9	12.3	52.1
10	4.6	5.4	0	5.1	25	59.9
11	3.2	3.8	2	17.5	17.5	56
12	1.7	2.2	3.7	5.4	9.9	77.1
13	3.2	3.8	0.2	30	17.5	45.4
14	4.5	5.2	3.6	5.8	24.5	56.4
15	4.6	5.4	2	5	25	58

mainly of equal amounts of orthoclase and albite. The oxide compositions given in Table 2 were statistically chosen within the field of interest for floor tiles and sanitaryware. This way of choosing the composition offers a possibility to establish models for predicting the compositional dependence of properties.

The glaze suspensions were applied on green floor tiles in a waterfall-coating process and then fired in three different ways: (1) industrial fast-firing with top temperature 1215 °C and a total

firing cycle of 60 min, (2) traditional firing in a laboratory furnace (Naber Labotherm N60 HR) with top temperature 1215 °C and a total firing cycle of 24 h, and (3) intermediate firing cycle in a laboratory furnace (Carbolite RHF 16/35) with top temperature 1260 °C and a total firing cycle 450 min. The industrial firing and the intermediate firing give the same porosity for the tiles. The phase composition of the glazes was analyzed with X-ray diffraction (X’pert by Philips) and with scanning electron

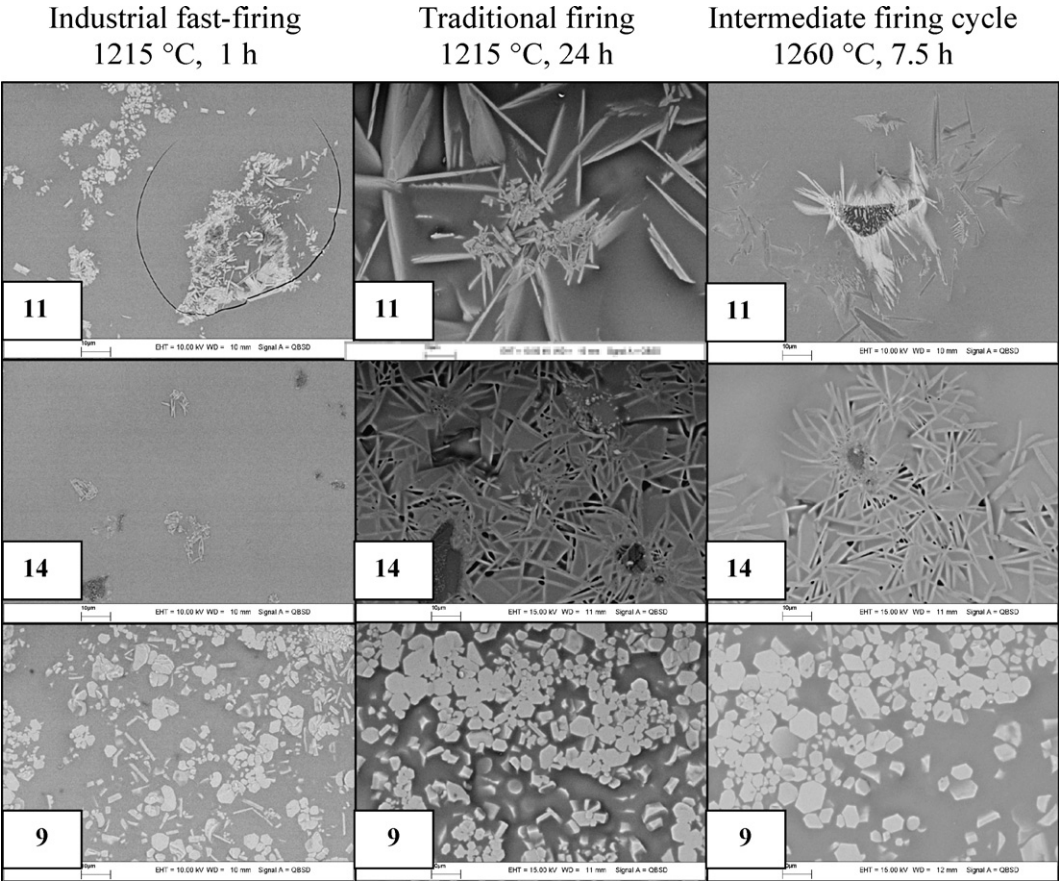


Fig. 1. SEM images of the crystalline phases after (1) fast-firing: glaze 11 wollastonite, glaze 14 diopside, glaze 9 pseudowollastonite; (2) traditional firing: 11 wollastonite, 14 feldspar, 9 pseudowollastonite; (3) intermediate firing: 11 feldspar + wollastonite, 14 feldspar, 9 pseudowollastonite.

microscopy equipped with electron dispersive X-ray analysis (SEM/EDXA, LEO 1530 by Zeiss/Vantage by Thermo Electron Corporation).

The raw material reactions were studied by heating the samples in hot stage microscope (Misura 3.0 by Expert System) to several peak temperatures between 1000 and 1260 °C with a heating rate of 10 °C/min. Quenched samples from several peak temperatures were studied by SEM/EDXA for their phase composition.

3. Results and discussion

Different crystalline phases were developed in the glazes depending on their raw material composition and firing conditions. Fig. 1 gives the SEM images of three glazes fired according to the three cycles. According to XRD and SEM/EDXA analysis glaze 11 contains wollastonite and quartz after all firing cycles, and also feldspar crystals after the intermediate firing. Glaze 14 contains some diopside crystals around quartz particles and after the two other firing cycles feldspar was identified. Fast-firing of glaze 9 gives both wollastonite and pseudowollastonite crystals and mainly pseudowollastonite in the two longer firings.

Quartz and corundum were assumed to originate from unreacted raw materials and were mainly observed in the fast-fired glazes. In the fast-fired glazes also diopside, wollastonite and pseudowollastonite were identified. Fig. 2 gives the crystalline

phases for the experimental glazes in a simplified ternary phase diagram $\text{Al}_2\text{O}_3\text{--SiO}_2\text{--MO} + \text{M}_2\text{O}$ where the total sum of alkaline and alkaline earth oxides is given by $\text{MO} + \text{M}_2\text{O}$. The molar ratio magnesia to lime was found to control the crystal type: (1) $\text{MgO}:\text{CaO} > 0.2$ gives diopside, (2) $\text{MgO}:\text{CaO} \approx 0.2$ gives diopside and wollastonite in the same glaze, (3) $\text{MgO}:\text{CaO} < 0.2$ gives wollastonite, and (4) $\text{MgO}:\text{CaO} = 0$ gives pseudowollastonite. The amount of quartz also seems to influence on the precipitation of wollastonite and diopside. If quartz content was low, only diopside was observed thus suggesting that all the quartz available is consumed in diopside formation.

In glazes containing pseudowollastonite it remained as the main crystalline phase when the firing time was prolonged or when the temperature was increased, cf. Fig. 2(b) and (c). The main difference in the surface composition was the increased crystals size of the longer firing cycles, cf. glaze 9 in Fig. 1. In glazes with high magnesia and silica contents diopside was observed also for the both longer firing cycles. If the alumina content was high, mainly feldspar type crystals were observed as shown by glaze 14 in Fig. 1. This indicates that feldspar formation is favoured by high alumina, lime and magnesia contents, and its crystallization requires long firing cycles. The feldspar crystals identified were solid solutions of anorthite–albite in lime rich glazes, while in glazes with high magnesia content potassium feldspar–albite solid solution was observed. This suggests that the dissolution of lime in the feldspar rich melt favours

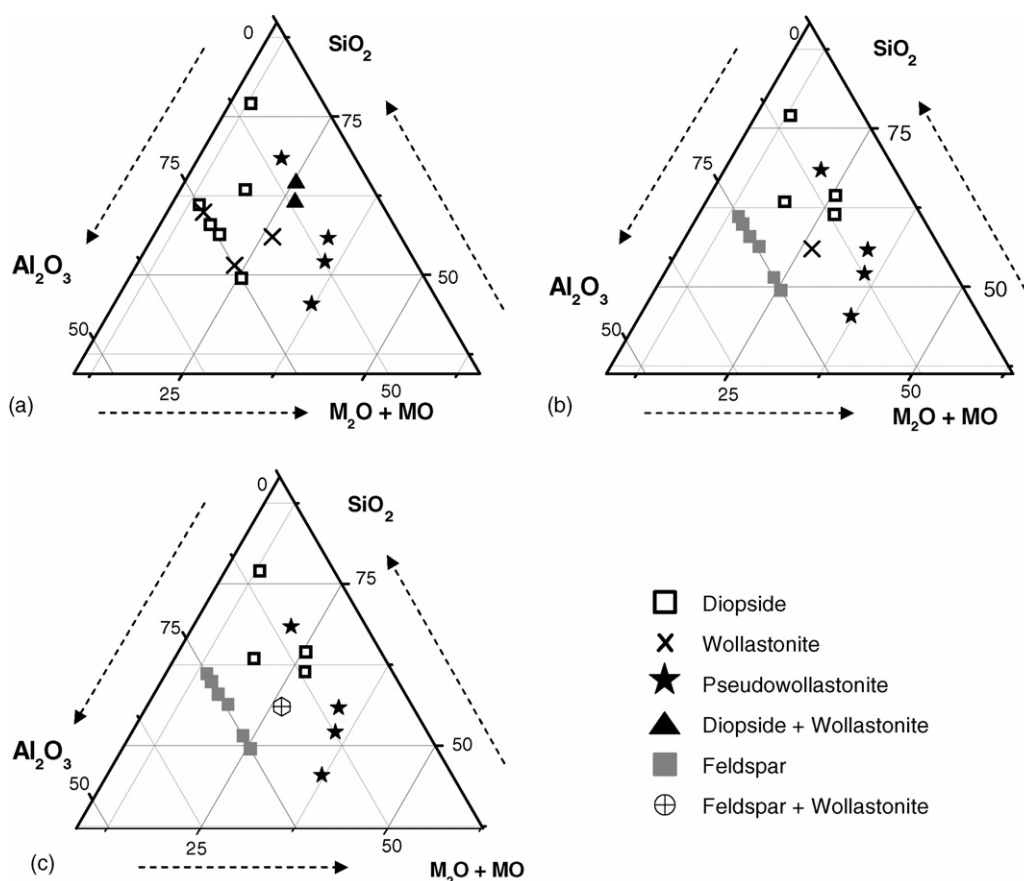


Fig. 2. Glaze composition (wt.%) and crystalline phases according to XRD and SEM/EDXA for the experimental glazes: (a) fast-firing; (b) traditional firing; (c) intermediate firing. $\text{M}_2\text{O} + \text{MO} = \text{Na}_2\text{O} + \text{K}_2\text{O} + \text{MgO} + \text{CaO}$.

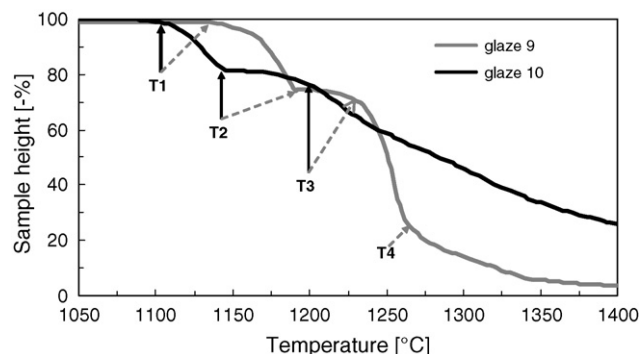


Fig. 3. HSM sintering curves showing sample height as a function of temperature for glazes 9 and 10. T_1 : onset of sintering, T_2 : onset of main reaction, T_3 : onset of melting, and T_4 : end of melting.

the formation of albite-type crystals, while the feldspar crystals in glazes with low lime content are predominantly typical of the feldspar raw material used, i.e. sodium–potassium feldspar crystals. The dissolution of wollastonite crystals at higher temperatures also seems to favour crystallization of feldspar.

Firing behaviour was studied as the influence of glaze composition on the sintering curve obtained with HSM. Fig. 3 shows the sintering curves, the decrease of the sample size as function of temperature, for glazes 9 and 10. The interpretation of the different phases of sintering was based on SEM images from samples quenched from several temperatures. These sintering phases were characterized by typical points in the HSM curve. Temperature T_1 given by the first permanent decrease in sintering curve was correlated with the commencement of sintering reactions. The onset temperature of the main sintering reactions was interpreted by T_2 as the ending of the first steep slope in the sintering curve. Onset of melting, T_3 was taken as the onset temperature of the second steep slope in the sintering curve. At temperature T_4 the glaze was almost completely melted and the curve height was assumed to be mainly controlled by the viscosity of the molten glaze.

The glazes started to sinter between 1030 and 1150 °C depending on the composition. The onset of sintering was mainly controlled by the contents of dolomite, limestone and feldspar. Regression analysis of the compositional dependence of T_1 on glaze raw material composition was calculated at a 95% significance level. The model

$$T_1 (^{\circ}\text{C}) = 1136.08 - 0.59p_{\text{feldspar}} - 1.81p_{\text{dolomite}} + 0.016p_{\text{limestone}}^2 \quad (1)$$

where p is the raw material in wt.%, has a regression coefficient $R^2 = 88.31\%$.

The main reaction started at 1140–1240 °C. According to the SEM images of the quenched samples this reaction correlated with the crystallization of diopside, wollastonite and pseudowollastonite. Accordingly the temperature depends on dolomite and limestone content as given by Eq. (2) with regression coefficient $R^2 = 92.06\%$

$$T_2 (^{\circ}\text{C}) = 1287.2 - 1.58p_{\text{feldspar}} - 2.45p_{\text{dolomite}} - 3.44p_{\text{limestone}} + 0.069p_{\text{limestone}}^2 \quad (2)$$

As the main reaction means crystallization, and thus formation of stoichiometric compounds, also oxide composition was found to give a good estimation of T_2 .

The model in Eq. (3) where p_i is the amount of the i th oxide in wt.%, has a regression coefficient $R^2 = 94.45$

$$T_2 (^{\circ}\text{C}) = 1303.89 - 23.44p_{\text{Na}_2\text{O}} - 5.95p_{\text{MgO}} - 6.38p_{\text{CaO}} + 0.18p_{\text{CaO}}^2 - 0.031p_{\text{Al}_2\text{O}_3}^2 \quad (3)$$

The temperature range for T_3 , the commencement of the main melting was 1160–1280 °C. This temperature partly correlated with the amount of crystals and no satisfactory model for the compositional dependence could be established. Also the interpretation of T_3 value was not unambiguous. The temperature was highest for glazes containing pseudowollastonite and lowest for compositions containing dolomite or limestone only. When these crystals were present simultaneously, the temperature was intermediate.

T_4 indicating the ending of the main melting was within 1210–1360 °C. The compositions of mat glazes suitable for fast-firing should have peak temperature between T_3 and T_4 . If the glaze has a small difference between these temperatures, variations in top firing temperature are likely to give differences in the surface phase composition. Glazes with the highest feldspar and quartz contents were found to give highest differences between T_3 and T_4 , obviously due to the high viscosity of the glassy melt.

The observations from the sintering curves were found to correlate well with the surface phase composition of fast-fired glazes. However, at longer cycles the phase conditions are likely to depend on the nucleation and growth of crystals in a more or less homogeneous melt of high viscosity.

4. Conclusion

The results indicate that firing conditions strongly influence the phase composition of glazes. In fast-firing quartz was not fully dissolved, while in longer firings the dissolution was complete. Diopside, wollastonite and pseudowollastonite were the main crystals observed in fast-fired surfaces. Longer firing times favoured the formation of feldspar, predominantly as anorthite–albite in lime rich compositions and potassium feldspar–albite in glazes low in lime. However, if the alumina content of the glazes was low, feldspar was not observed. Models for calculation of the compositional dependence of the temperatures indicating sintering and the main reactions were established. These models can be used to predict the conditions for fast-firing.

Acknowledgements

This work is part of the Activities of the Åbo Akademi Process Chemistry Centre funded by the Academy of Finland in their Centres of Excellence Programme. Financial support from the Clean Surfaces 2002–2006 Technology Programme by the Finnish National Technology Agency (Tekes), Graduate School of Materials Research, Ido Bathroom Ltd, Pukkila Oy Ab and Farnos is acknowledged. Ms Susanne Ena, Ms Jaana Paana-

nen and Mr Clifford Ekholm are thanked for their help with the analysis of the samples.

References

1. Achmed, M. and Earl, D. A., Characterizing glaze-melting behaviour via HSM. *Am. Ceram. Soc. Bull.*, 2002, **81**, 3.
2. Beyer, E. and Laniz, W., Hot stage microscopic studies of ceramic raw materials, pastes and glazes. *Silikattechnik*, 1972, **23**, 6.
3. Boccaccini, A. R. and Trusty, P. A., In situ characterization of the shrinkage behaviour of ceramic powder compacts during sintering by using heating microscopy. *Mater. Charact.*, 1998, **41**(4), 109–121.
4. Burzacchini, B., Paganelli, M. and Christ, H. G., Examination of fast-fire frits and glazes using a hot stage microscopy at different heating rates. *Ceram. Eng. Sci. Proc.*, 1996, **17**(1), 60–66.
5. Nikulina, L. K. and Pyzhova, A. P., Use of a hot stage microscope for studying glazes. *Neorg. Steklovidyne Prokrytiya Mater.*, 1969, 69–74.
6. Kronberg, T., Hupa, L. and Fröberg, K., Modelling of firing behaviour of raw glazes. *Adv. Sci. Technol.*, 2003, **34**, 55–62 [Science for New Technology of Silicate Ceramics].
7. Paganelli, M., Using the optical dilatometer to determine sintering behaviour. *Am. Ceram. Soc. Bull.*, 2002, **81**(11).
8. Paganelli, M., Understanding the behaviour of glazes: new test possibilities using the automatic hot stage microscope “MISURA”. *Ind. Ceram.*, 1997, **17**(2), 69–73.
9. Paganelli, M., In situ observation of ceramic tiles body batches sintering in fast firing cycles. *Ind. Ceram.*, 1996, **16**(1), 1–6.
10. Siligardi, C., D’Arrigo, M. C. and Leonelli, C., Sintering behaviour of glass–ceramic frits. *Am. Ceram. Soc. Bull.*, 2000, **79**(8), 88.
11. Rincon, J. M., Romero, M., Marco, J. and Caballer, V., Some aspects of crystallization microstructure on new glass–ceramic glazes. *Mater. Res. Bull.*, 1998, **33**(8), 1159–1164.
12. Alptekin, K. and Kara, F., Glass ceramic glazes in the CaO–SiO₂ system. *Key Eng. Mater.*, 2004, **264–268**, 1709–1712.
13. Baldi, G., Generali, E., Leonelli, C., Manfredini, T., Pellacani, G. and Siligardi, C., Effects of nucleating agents on diopside crystallization in new glass–ceramics for tile-glaze application. *J. Mater. Sci.*, 1995, **30**(12), 3251–3255.
14. Övecoglu, M. L., Kuban, B. and Özer, H., Characterization and crystallization kinetics of a diopside-based glass–ceramic developed from glass industry raw materials. *J. Eur. Ceram. Soc.*, 1997, **17**, 957–962.
15. Zdaniewski, W., DTA and X-ray analysis study of nucleation and crystallization of magnesia–alumina–silica glasses containing zirconia, titania and cerium (IV) oxide. *J. Am. Ceram. Soc.*, 1975, **58**(5/6), 163–169.
16. Zdaniewski and Wieslaw, A., Microstructure and kinetics of crystallization of magnesium oxide–aluminium oxide–silicon dioxide glass–ceramics. *J. Am. Ceram. Soc.*, 1978, **61**(5/6), 199–204.
17. Leonelli, C., Manfredini, T. and Paganelli, M., Crystallization of some anorthite–diopside glass precursors. *J. Mater. Sci.*, 1991, **26**, 5041–5046.
18. Sainamthip, P. and Reed, J. S., Glazes for fast-fired wollastonite wall tile. *Am. Ceram. Soc. Bull.*, 1989, **68**(1), 103–106.
19. Kokubo, T., Bioactive glass ceramics: properties and applications. *Biomaterials*, 1991, **12**(2), 155–163.
20. Fokin, V. M., Nascimento, M. L. and Zanotto, E. D., Correlation between maximum crystal growth rate and glass transition temperature of silicate glasses. *J. Non-Cryst. Sol.*, 2005, **351**(10/11), 789–794.